Journal of Glaciology, Vol. 39, No. 133, 1993

Siple Coast Project research of Crary Ice Rise and the mouths of Ice Streams B and C, West Antarctica: review and new perspectives

ROBERT BINDSCHADLER
NASA/Goddard Space Flight Center, Code 971, Greenbelt, Maryland 20771, U.S.A.

ABSTRACT. Satellite imagery is used as a basis to review and critique the results of studies at the mouths of Ice Streams B and C and Crary Ice Rise. In many cases, these past analyses are extended by taking advantage of the broad coverage within each image. New perspectives are provided by the image data and some long-standing controversies are resolved. The grounding line is easily delineated and mapped in areas covered by imagery. Extensive areas of grounded ice with complex patterns of flow stripes are identified on the flanks of Crary Ice Rise. The imagery also allows a corrected map of surface topography in the vicinity of the Downstream B camp. New questions are posed by hitherto unseen features. Data from the IGY traverse of the Ross Ice Shelf in 1957 are included to demonstrate that large changes have occurred in the past almost 30 years in the area upstream of Crary Ice Rise. These changes include modifications in the surface topography, elimination of crevasses and increases in the ice thickness by approximately 60 m.

INTRODUCTION

The Siple Coast Project (SCP) began in 1983 as a set of separate investigations on Ice Streams B and C to study ice-stream behavior and the interaction between the ice streams and the Ross Ice Shelf. Individual investigators quickly recognized their common interests and a set of three goals was agreed upon: to determine the configuration and mass balance of the West Antarctic ice streams feeding the Ross Ice Shelf, to determine the physical controls on ice flow in this region, and to predict the future behavior of the region through the development and application of numerical models (SCP, 1989). These goals formed the scientific framework of the Siple Coast Project. With these goals as a collective objective, investigators exhibited close co-operation in the sharing of logistic resources, scheduling of field activities, types and location of field experiments and, most importantly, exchange and collaborative analyses of data. The results have been published in an extensive collection of papers in a variety of journals and a concise review has been written by Alley and Whillans (1991).

Much of what was learned during the Siple Coast Project resulted from data collected at the mouth of Ice Streams B and C, on the ice plain of Ice Stream B, and around Crary Ice Rise (Fig. 1). The general purpose of the studies in this region was to understand the interaction between the Ross Ice Shelf and the ice streams. The objective was based on published theories that the ice shelf was instrumental in determining the flow of the grounded ice sheet (Hughes, 1973; Thomas, 1973). These theories held that the back pressure caused by the friction of the ice shelf generated at localized grounded regions and along the ice-shelf sides prevented a rapid collapse of the ice sheet. Furthermore, if either rising sea level or thinning of the ice shelf occurred (caused by increased basal melting), this back pressure would decrease and there would be the increased danger of ice-sheet collapse. While the measurements of the lower ice-stream/ice-shelf region have succeeded in quantifying that there is an important, but not dominant, effect of the ice shelf on the ice-stream system (MacAyeal and others, 1987), they have allowed a number of additional discoveries leading toward quite a different view of the nature of ice flow in this region. Most startling are the numerous illustrations of dramatic changes taking place on sometimes very short time-scales (Stephenson and Bindschadler, 1988; Bindschadler and others, 1989, 1990).

This paper will review the dynamics of the region of the West Antarctic ice sheet but will include analysis of more recently acquired SPOT (Satellite Pour l'Observation de la Terre) imagery of the area (see Fig. 1). The review serves to conclude and summarize the SCP studies in this area—the image data serve to introduce additional analyses that bear directly on many of the earlier published results. In some cases, the image analysis supports or confirms earlier hypotheses; however, in other cases, the imagery indicates that modifications to published work are required.

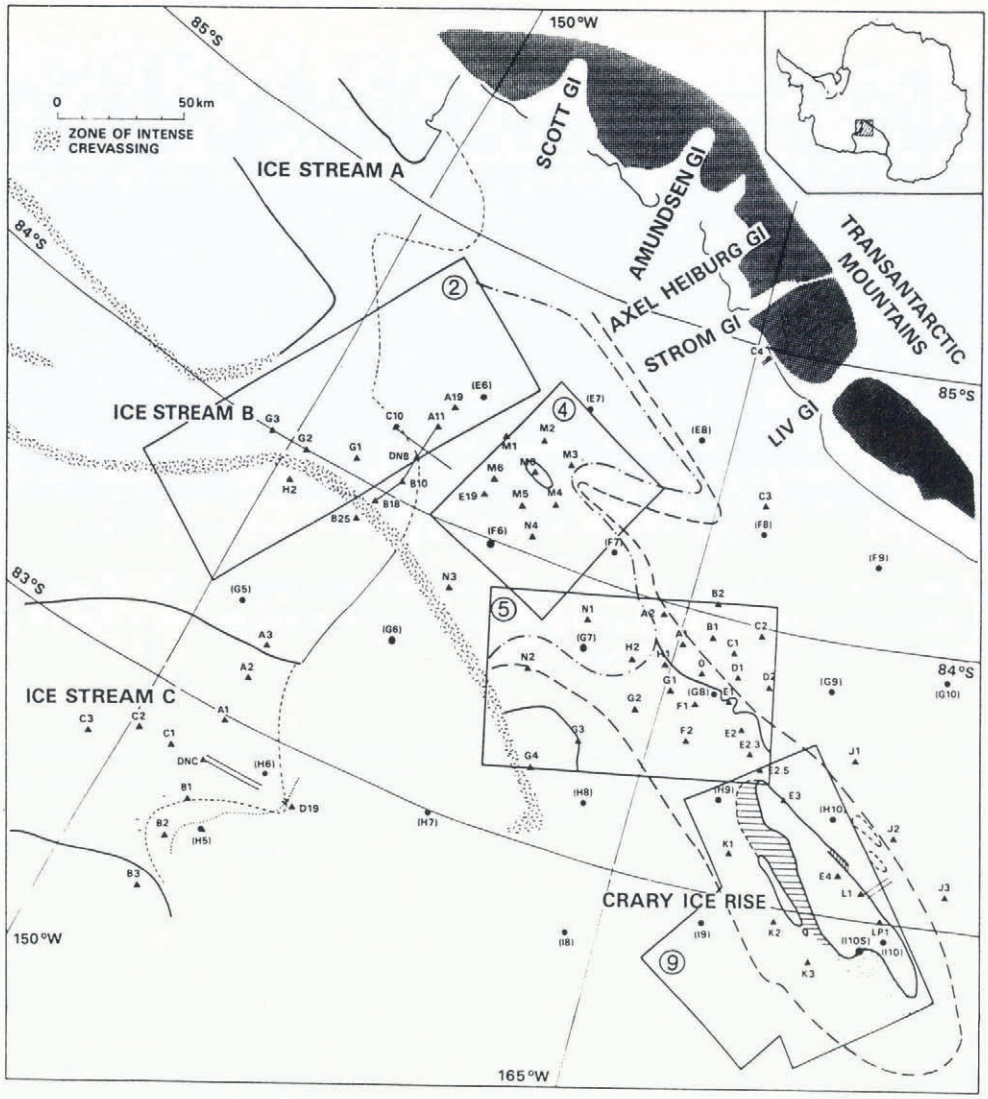

Fig. 1. Map of the study area. Solid triangles and names are SCP stations, solid circles and names in parentheses are selected RIGGS stations. Positions of SPOT scenes are outlined and identified by circled number which gives their figure number. Grounding-line positions are shown by the following lines: light dashed, Rose (1979); dotted, Bindschadler and others (1987b); dash-dotted, Bindschadler and others (1987a); heavy dashed, Shabtaie and Bentley (1987); and heavy solid, this paper. Figure adapted from Bindschadler and others (1987a).

DOWNSTREAM B AREA

The SCP field work began at a camp located in the mouth of Ice Stream B in November 1983. The camp position was chosen to coincide with the grounding line as mapped by Rose (1979). The major aims of the work in this area were to determine the mass discharge of the ice stream at the grounding line, to measure the deformation in the flow and to learn more about the interaction between the ice stream and the ice shelf.

An optically continuous line of stakes across the mouth of Ice Stream B was established for the discharge and deformation measurements. This line extended from a point north of the active ice stream (B25), past the Downstream B (DNB) camp, to a point in the flow of Ice Stream A (A19) (see Fig. 1). The velocity along this profile showed that the flow was almost plug-like across most of the ice stream with velocity variations of only a few per cent (see Bindschadler and others, 1987a, fig. 7). Combined with airborne radar measurements of the ice thickness (Shabtaie and others, 1988), this profile has provided an extremely important measure of the discharge flux from Ice Stream B for the calculation of net mass balance (Bindschadler and others, 1987a; Shabtaie and others, 1988; Whillans and Bindschadler, 1988). All these papers have concluded that the net mass balance of Ice Stream B above this profile is negative. The last paper supplies the most accurate assessment: a 40% negative balance.

The character of plug flow measured at the DNB profile is in strong contrast to the more variable velocity field measured over a part of Ice Stream E (Bindschadler and Scambos, 1991). The Ice Stream E velocities were measured from sequential satellite images at a place well upstream of the grounding line. Variations of up to 25% were discovered and correlated with the pattern of surface undulations. The spatial stability of these undulations was established by these authors and they inferred that the undulation field is correlated with basal topography. If this is true, then it is the bed relief that forces the pattern of the velocity field through variations in the form drag. MacAyeal (1992) has developed an inverse method based

https://doi.org/10.3189/S0022143000016439 Published online by Cambridge University Press

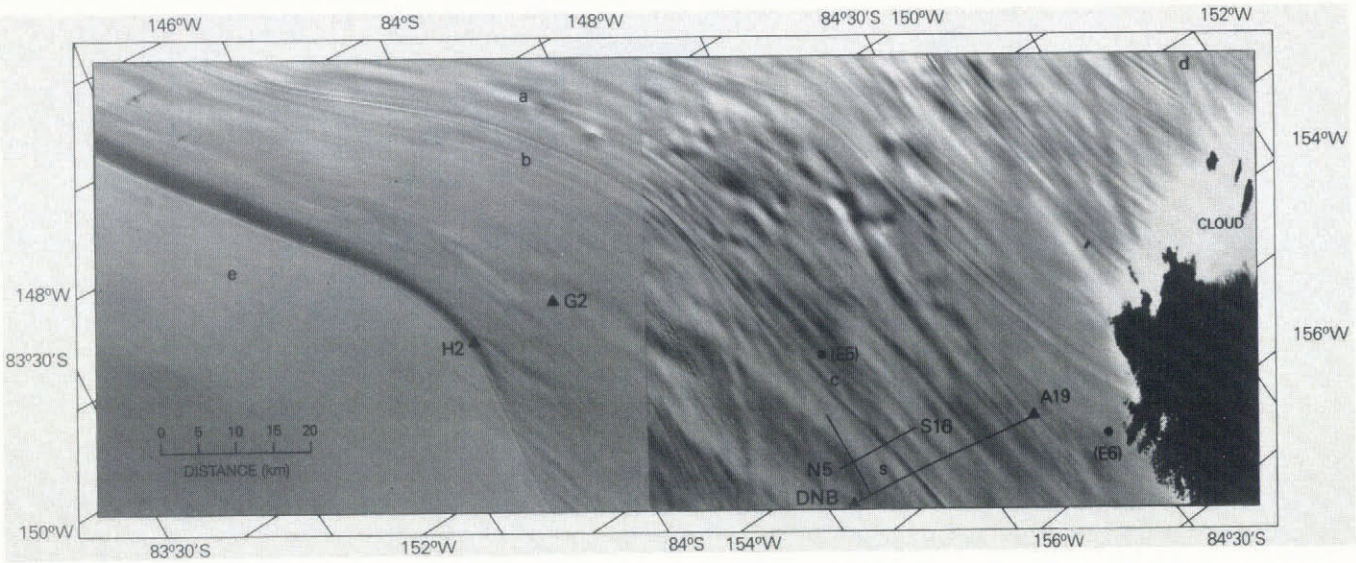

Fig. 2. Mosaic of two SPOT scenes of Ice Stream B. Solid circles and triangles are RIGGS and SCP stations, respectively. Solid lines are level lines. Elevations along two parallel transverse lines are shown in Figure 3. Letters "a" through "e" and "s" refer to features discussed in the text.

on control theory to derive the pattern of basal shear from the surface velocity and has shown that the basal shear varies in such a way as to confirm the hypothesis of Bindschadler and Scambos (1991).

Figure 2 is a mosaic of two SPOT images taken of an area which includes a part of the DNB profile. It shows that the profile extends across a crevasse-free region devoid of major undulations. Thus, plug-like flow is expected. Farther upstream and to the south (the upper part of the figure), undulations are more plentiful and some crevasses can be seen; both are indicators of a more variable velocity field.

Because the reflectance of the snow surface is extremely homogeneous, there is a strong correlation between image brightness and surface slope in the direction of the Sun's illumination (Rees and Dowdeswell, 1988; Vaughan and others, 1988). The correlation is confirmed here by the elevation measurements made along the transverse profile passing through DNB and the parallel profile 5 km upstream (N5–S16), shown in Figure 3a and b, that cross a series of "flow stripes" with peak-to-trough amplitudes of a few meters. Steep south-facing slopes match bright image pixels while north-facing slopes correspond to darker pixels.

The high-resolution image of Figure 2 provides an excellent view of the flow stripes even though the Sun's illumination is not parallel to the leveling lines nor are these lines orthogonal to the flow stripes. This is because the flow stripes are the dominant shorter-scale topographic signature in this area. Less apparent in the image are the longer-scale topographic variations, e.g. the 16 m rise over 14 km between stations A19 and DNB (cf. Fig. 3a). The combination of image and leveling data is synergistic and leads to a correction of the earlier interpretation of surface topography in the vicinity of DNB (see Bindschadler and others, 1987b, fig. 8). Figure 3c presents a revised interpretation of the approximately 75 km of leveling data that is consistent with the brightness patterns in the image. The earlier interpretation incorrectly matched elevations between leveling lines, producing a lineated topography rotated approximately 45° from the correct orientation.

This more correct topographic map solves the difficulty in interpreting the pattern of surface strain rates measured along the longitudinal line at DNB (Bindschadler and others, 1987b, fig. 9). With the ridge axis now aligned nearly east–west, the principal compressional axis lies parallel to the ridge axis, and the principal tensile axis is orthogonal to the flow stripes. This strain-rate pattern expresses the reduction in speed and the lateral divergence experienced by the ice as it enters the mouth of Ice Stream B.

Bindschadler and others (1987a) also used their measured strain rates to conclude that the lifetime of the topographic variations must be short and, therefore, locally generated. That statement was based on a calculation which showed that the transverse strain rates measured at the surface were strongly correlated with the topography and were large enough to smooth out these topographic variations rapidly. This result applied best to the longer wavelength features, which can now be identified in the image as features such as the 4–6 km wide feature marked "s" in Figure 2. The longer wavelength features appear similar to those identified as spatially fixed on Ice Streams D and E. Thus, their "local generation" is probably due to subglacial relief, and the strain rates measured on the ice surface above them reflect the response of the ice as it flows over these permanent bed features. Conformation of the ice surface to bed features implies that, in some sense, the bed is "harder" than the ice, as pointed out by C. R. Bentley (personal communication). At first, this may seem to contradict the belief that ice streams are underlain by a pervasive layer of soft, deformable till (Alley and Whillans, 1991) but the till is a relatively thin layer (a few meters) and the bed features expressed in the surface topography exist on a much larger scale.

The correlation of surface topography and ice thickness published by Bindschadler and others (1987a, fig. 5) confirms that surface relief on a horizontal scale of

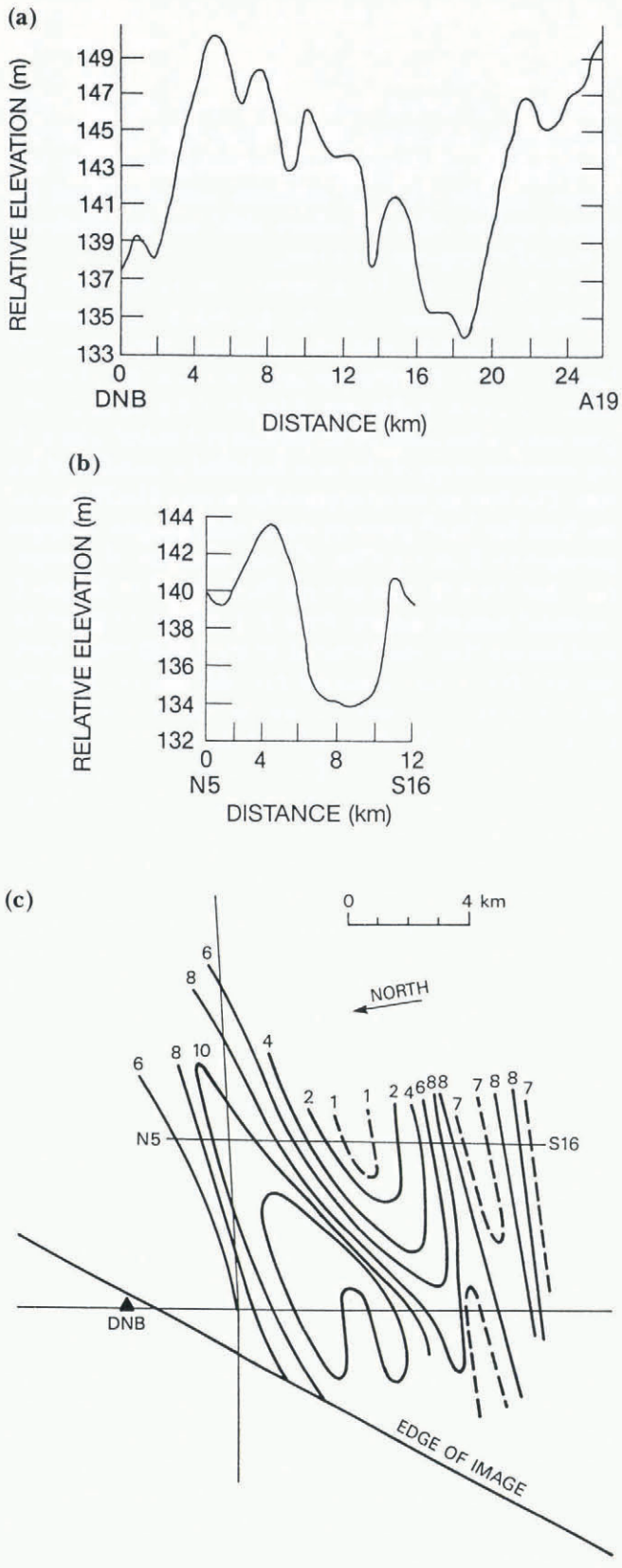

Fig. 3. Relative elevation profiles in the vicinity of DNB camp (cf. Fig. 2). (a) Station DNB to station A19; (b) short line parallel to (a) and 8 km upstream; (c) contour map of relative surface topography (2 m intervals) based on leveling data collected along three lines indicated in figure. Contour map corrects Bindschadler and others (1987b, fig. 8); both maps are consistent with level data but interpretation presented here also is consistent with image data. Level data were collected every 250 m along each profile. Data are taken from Bindschadler and others (1988b).

a few kilometers does correspond, in a subdued fashion, with the subglacial relief. Conversely, the strain rates for the shorter wavelength features, which can now be identified as the flow stripes, were lower, indicating a longer lifetime. Appropriately, the image shows that they do persist much longer than the large features.

There are two very prominent flow stripes in Figure 2. The first passes through station E5 and corresponds to the trace of the confluence of the two major tributaries of Ice Stream B (usually referred to as "B1" and "B2") which occurs approximately 150 km upstream. The second prominent flow stripe is seen entering Figure 2 at the middle of the top ridge and leaving the righthand edge under the cloud shadow (south of station E6). This flow stripe is formed upstream at the confluence of Ice Streams A and B. The prominence of these boundaries is very useful in defining the course of each ice stream and its tributaries out on to the ice shelf. Their persistence may be due to peculiarities in their rheology created at the generating confluence. The few measurements of surface strain rate on or near the septum between B1 and B2 are among the lowest anywhere in the mouth of the ice stream (Bindschadler and others, 1987a, fig. 9).

A variety of flow stripes fills the image area. Although the flow stripes tend to extend over large distances, there are numerous places where they can be seen beginning and ending. Often their generation is associated with an undulation but not always. An example of the generation of a flow stripe is seen in the upper part of Figure 2 (marked "a"). Not all flow stripes parallel the flow direction—some have twists or deflections, or they begin adjacent to the termination of another (see "b" and "c" in Figure 2). The chevron pattern in the upper right of Figure 2 (marked "d") is particularly peculiar. It is difficult to see how any flow stripe could have been formed in an orientation other than the flow direction at the time it was generated, but a changing flow pattern could cause it to deviate considerably from the present flow direction. MacAyeal and others (1988) have used a numerical model of ice-shelf flow to show how these deviations could develop and evolve.

Other features, seen in clusters near the center of Figure 2, have been referred to as "snow mounds"—mounds of wind-packed snow whose formation has been hypothesized as being related to wind flow in the vicinity of crevasses (Vornberger and Whillans, 1986). They always appear together with crevasse fields and they exhibit a "tail" of material that expresses the prevalent downwind direction.

The region of most intense crevassing (called the "snake") marks the north margin of Ice Stream B. Crevassing is so intense in this band that the numerous voids cast shadows that cause a noticeable darkening of the image brightness. The snake turns as the ice stream widens and the velocity decreases, reducing shear stresses at the margin. Fewer crevasses form, existing crevasses widen less rapidly, and snow fills each more rapidly per distance traveled. All these processes tend to reduce the shadowing apparent in Figure 2 on the more downstream parts of the snake.

Of the many undulations that are seen in Figure 2, most are elongated in the direction of flow. On the ridge, called Ridge BC, adjacent to the ice stream, there is a

https://doi.org/10.3189/S0022143000016439 Published online by Cambridge University Press

series of subtle undulations (marked "e") which parallels the snake. The appearance of undulations near the stream margins on inter-stream ridges is common (Bindschadler, unpublished) and is probably related either to the decrease in ice thickness as the margin is approached or to an increase in ice velocity. Both processes will create a situation where bed roughness is more effectively expressed in the surface topography. These undulations maintain an orientation parallel with the snake until the snake turns (near station H2), at which point the undulations intersect the snake and reappear at the same orientation within the ice stream itself. This lineation is probably an expression of a bed formation that may influence the flow direction of the ice stream for some distance but, eventually, other factors cause the ice stream to cut across this formation.

ICE PLAIN

One of the earliest surprises in the DNB studies was that the DNB camp was nowhere near the grounding line. Rose's (1979) determination of the grounding-line position was based on the surface elevation and ice thickness, both derived from airborne-radar soundings collected in the 1970s. By applying the criteria of a change in surface slope and ice thickness above buoyancy to discriminate between grounded and floating ice, the grounding line should have been near DNB. Our SCP field surveys of elevation, searching for large changes in surface slopes, measurements by tiltmeter (Stephenson and Doake, 1982) and searches for strand cracks all failed to provide conclusive identification of the grounding line.

Through a number of avenues of analysis, it was eventually recognized that there was a region of very slightly grounded ice extending more than 100 km downstream from DNB and that the change in surface slope identified by Rose represented a dynamic boundary between grounded and very slightly grounded ice, rather than between grounded ice and floating ice (Shabtaie and Bentley, 1987). This new boundary has been termed the "coupling line" (Alley and others, 1989). Bindschadler and others (1987a) calculated that the average basal shear stress over this region, called the "ice plain", was only 0.44 ± 0.5 kPa (0.0044 ± 0.005 bar) with elevations above buoyancy of only 30–40 m.

Because the grounding line was initially believed to be much farther upstream than it truly is, most measurements of surface strain on the ice plain were made with a scheme appropriate for floating ice. This fact explains what had been a baffling set of highly variable strain rates that defied simple interpretation (Bindschadler and others, 1987a). The measured strain rates indicate local strain rates induced by slight, but relatively important basal stresses, which are absent on ice shelves. As mentioned above, these strain rates operate to smooth the ice surface quickly once the ice becomes afloat.

The existence of the ice plain is due to the formation of a till delta formed by the flow of Ice Stream B. Blankenship and others (1987) inferred, and later Engelhardt and others (1990) confirmed, that Ice Stream B is underlain by a water-saturated, highly deformable bed. A deforming-bed hypothesis for ice-stream motion leads to the prediction of an ice-plain-like structure at the mouth of the ice stream with the underlying sediments of a till delta stratified in a succession of foreset beds (Alley and others, 1989; Blankenship and others, 1990). These beds are built up by deposition of subglacial till resulting from past ice-stream motion. This till structure was confirmed by seismic studies (Alley and others, 1989) and lent credence to the deforming-bed hypothesis.

Recognition of the grounded ice plain and the associated mislocation of the grounding line created numerous conflicts with the previous analyses of the Ross Ice Shelf. Foremost among these was the classification of ice rises in this area. Clearly, if the ice plain was grounded, there could be no ice rises embedded within it, but previous maps of this area included a number of ice rises. The first ice rise to appear did so on a USGS map of the Ross Ice Shelf based on aerial photographs. Oblique photograph F-33-1-2-172#130 was taken on 13 November 1966, looking downstream from over Ice Stream B (personal communication from R. J. Allen). It shows an oval feature that was included in the USGS map. Jezek and Bentley (1983) indicated that this feature, between RIGGS stations F6 and F7, was an ice rise which they labeled ice rise "A". They inferred the positions of many other ice rises on the ice shelf from the presence of bottom-crevasse signatures in radar data collected during RIGGS. Their ice rise located just downstream of RIGGS station G6 (see Fig. 1) and labeled ice rise "B" is almost certainly false, this area being an open rift in the ice shelf at the termination of the snake (discussed later). In still another interpretation, Shabtaie and Bentley (1987) retained the ice rise "A", and added a second centered on SCP station M0. The existence of this second ice rise, labeled ice rise "a", was based on the identification of a radar-sounding signature characteristic of ice rises (Shabtaie and Bentley, 1987). Thus, multiple-data sources and poor navigation led to a controversy over how many such features actually existed.

Figure 4 is a SPOT image that clearly shows ice rise "a", the nearly oval feature coincident with SCP station M0. The flow stripes indicate flow around the feature, but velocity measurements made at M0 ($471 \pm 7\,\mathrm{m\,a^{-1}}$) and at the nearby stations E19 ($465 \pm 8\,\mathrm{m\,a^{-1}}$) and M3 ($470 \pm 7\,\mathrm{m\,a^{-1}}$) show that to the limit of the measurements, "a" is traveling at the same velocity as the surrounding ice (Bindschadler and others, 1987a). Alley (1993) has remarked that the uncertainties in the velocities allow for the possibility that flow around "a" is the current flow pattern. Surface strain rates measured at all the stations surrounding "a" and at station M0 revealed a complex pattern inconsistent with shearing past "a" (Bindschadler and others, 1987a). However, because the ice is grounded everywhere within this image, the measured strain rates are strongly influenced by the local stresses and are less related to the regional stress field. Thus, the existing measurements may not be spaced tightly enough to detect the localized flow pattern proposed by Alley.

Because "a" is not surrounded by floating ice shelf, it cannot be an ice rise and it is now called "ice *raft* 'a' ". From both the character of the flow stripes defining this feature and its radar signature, it is concluded that this

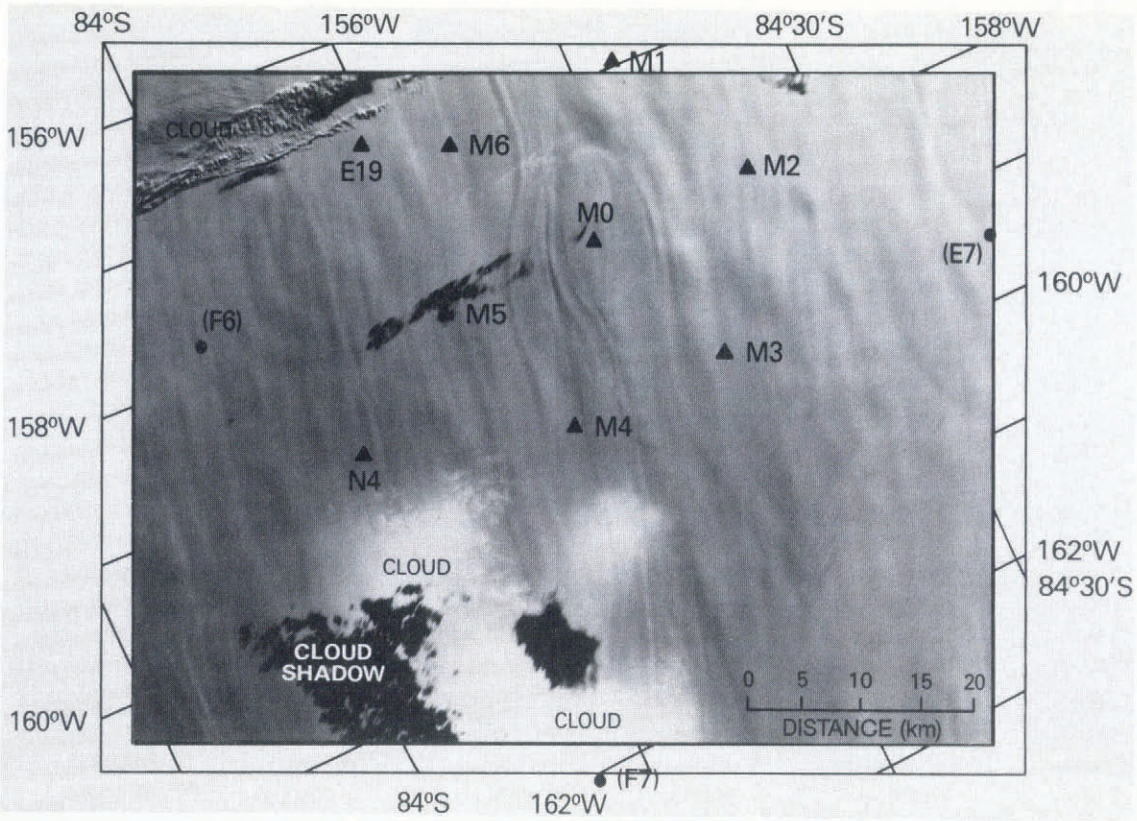

Fig. 4. SPOT scene of ice raft "a". RIGGS and SCP stations are identified.

feature was once a grounded ice rise surrounded by an ice shelf which flowed around it. By some means, and at some unknown location upstream, this feature became dislodged and it is now flowing downstream. Surface-leveling data show that station M0 lies 15 m above station M3 but at the same elevation as station M6 (unpublished data of R. Bindschadler). Ice raft "a"'s location coincides with a region of thinner ice implying a higher bed elevation than elsewhere on the ice plain (Shabtaie and Bentley, 1988). A detailed map of current rates of thickness change in this region calculates rapid thickening upstream of "a" and rapid thinning downstream (Bindschadler and others, 1993). This result, combined with the measurement of very small surface strain rates in this area (Bindschadler and others, 1987a), suggests that the high spot in the underlying bed is moving downstream along with the surface feature. A similar movement near the grounding line of Rutford Ice Stream has been documented by Vaughan and Doake (1989).

Figure 4 does not conclusively dismiss the existence of ice rise "A". Its position on the USGS map lies between RIGGS stations F6 and F7 and very near SCP station N4, but the navigational accuracy of the aircraft can be questioned and the similarity in shape between the feature in that photograph and ice raft "a" strongly suggests that they are the same feature. Nevertheless, it is possible that some smaller feature lies under the cloud in Figure 4. On either side of this cloud (the very bright area) and its shadow (the very dark area); flow stripes that turn inward toward the obscured area can be seen. Subsequent images of this area will be the only certain means of determining the presence or absence of a second feature.

Figure 5 is a mosaic of two SPOT scenes which extend the coverage farther downstream on the ice plain and force major revisions to much of what had been deduced from field measurements. The distinction between grounded and floating ice is quite apparent over most of these two images and illustrates that the ice plain (i.e. the grounded ice) extends over an even larger area than previously mapped (see Fig. 1). The smoothness of the ice-shelf surface is a result of the rapid equilibration of small-scale surface-slope variations. The ability to distinguish between grounded and floating ice based on this topographic characteristic has been confirmed by Jacobel and Bindschadler (1993).

The grounding line appearing in Bindschadler and others (1987a) was drawn between SCP stations G2 and H2, and separated the ice plain from Crary Ice Rise. This interpretation was based largely on the deductions that G2 was floating and that a level line between these two stations crossed the grounding line (Bindschadler and others, 1987a, fig. 3). Later analysis showed the surface elevation of G2 to be above hydrostatic equilibrium (Bindschadler and others, 1988b). Thus, Shabtaie and Bentley's (1987) interpretation that extended the ice plain downstream to Crary Ice Rise appears correct.

The left part of Figure 5 clearly shows the grounding line and indicates that the grounding line published by Shabtaie and Bentley (1987) is placed too far upstream. Bindschadler and others (1987b) reported SCP stations G3 and G4 were both floating (based on 1984 data). Figure 5 indicates that G3 is sited within a small embayment just on the floating ice. Surface-leveling data collected in the 1988–89 field season, between G2 and G3, show a steep surface slope very near G3, lending strong support to this interpretation.

https://doi.org/10.3189/S0022143000016439 Published online by Cambridge University Press

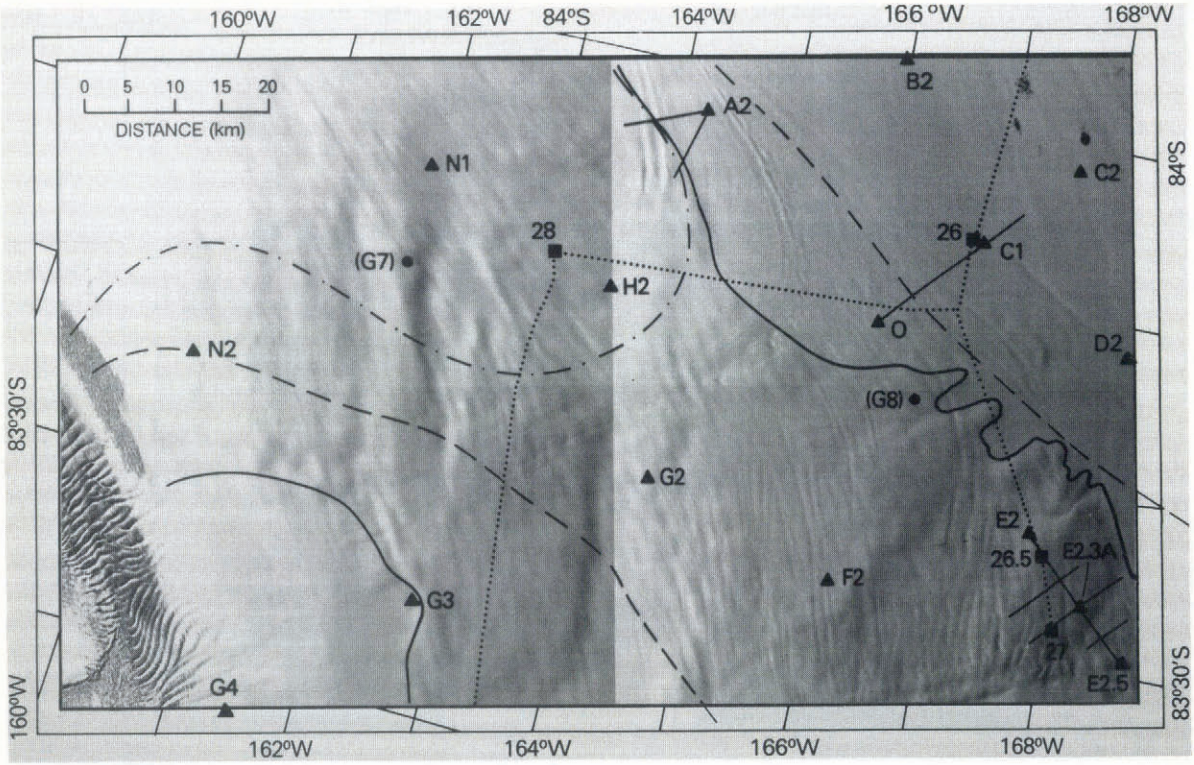

Fig. 5. Mosaic of two SPOT scenes in ice-plain region. Solid circles, triangles and squares are stations from RIGGS, SCP and IGY, respectively. Straight solid lines are level lines. Dot-dash, long-dash and solid lines are grounding-line positions from Bindschadler and others (1987a), Shabtaie and Bentley (1987) and these images, respectively. Dotted line is IGY traverse route (Crary and others, 1962).

The grounding-line position is least apparent in the vicinity of SCP station A2 (see Fig. 5) and probably strikes parallel to the direction of the Sun (upper left). Fortunately, this is the area where the field data of the grounding line are most certain. Measurements of surface elevation and ice thickness and the observation of strand cracks along two profiles from station A2 are definitive (Bindschadler and others, 1987a). Figure 6a and b present the relative elevation profiles along these two transects, and their positions are indicated in Figure 5 (Bindschadler and others, 1988b). The elevation profiles agree very well with the topography as indicated in the image. The two bright bands crossed by the profile in Figure 6b were generated as a single flow stripe at the downstream end of ice raft "a" (see Fig. 4).

The grounding line between A2 and Crary Ice Rise is shown in Figure 5 to be irregular but it agrees roughly with the grounding line published by Shabtaie and Bentley (1987). By coincidence, a number of stations (both RIGGS and SCP) are positioned very near the grounding line. Stations O and C2 are floating as reported by Bindschadler and others (1987b). At RIGGS station G8, Robertson and Bentley (1990) published a water depth of 89 m based on seismic measurements made in 1973, but Bentley (personal communication) now cautions against assigning much confidence to this measurement. As argued later, however, it is likely that the grounding at G8 is recent, occurring after the RIGGS measurements in 1973. Post-RIGGS grounding would be consistent with the discovery of Stephenson and Bindschadler (1988) that the ice velocity at this location has slowed by 16% during the 11 years between RIGGS and SCP.

Between RIGGS station G7 and SCP station H2, there is a large depression of uniform brightness in the ice plain close to G7 (the Sun illumination is from the upper left). The most obvious interpretation of this feature is that it is an isolated area of floating ice within the ice plain.

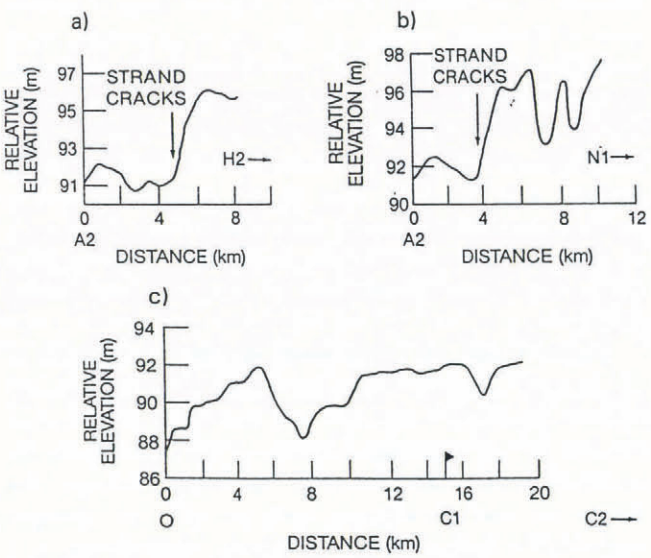

Fig. 6. Relative elevation profiles in vicinity of grounding line and marked on Figure 5: (a) station A2 toward station H2; (b) station A2 toward station N1; and (c) station O toward station C2. Positions of observed strand cracks are indicated. Level data were collected every 250 m along each profile. Data are taken from Bindschadler and others (1988b).

There is a second set of curving, nearly parallel flow stripes entering Figure 5 just above station A2 (at 164° W). These, too, are related to ice raft "a" and exit Figure 4 just to the right of the clouds. Downstream of A2, they sweep transversely across the direction of flow on the ice plain (approximately 300° true). The thicker of these bands is also highly variable in width, even discontinuous in places. The flow stripes are reminiscent of a band of surface moraine on a valley glacier that is elongated near the shear margin. On the ice plain, there is no comparable shear margin but in the past, when ice raft "a" was grounded, there might have been. This is also the area where bottom crevasses were detected with sounding radar (Jezek, 1984). The location uncertainty of the aircraft used in the radar survey makes the precise positioning of these crevasses impossible, but the approximate position falls between RIGGS station G8 and SCP station A2. Given the close correspondence between ice rises and bottom crevasses (Jezek and Bentley, 1983), it is likely that there is a continuous trail of bottom crevasses from this point upstream to ice raft "a". Unfortunately, radar data do not exist to confirm this hypothesis. The distance between "a" and the downstream end of this feature is roughly 100 km, or roughly 200 years, assuming a stationary "a" and a velocity of 500 m a^{-1} for ice on the ice plain.

Detailed surface work was also carried out in the region of SCP stations E2, E2.3A and E2.5, located in the lower right of Figure 5. Radar soundings collected throughout this area by a surface-based system showed no variation in ice thickness (personal communication from S. Shabtaie). Thus, the surface relief seen in the imagery is close to a direct reflection of basal relief. The single snow mound near the southwest end of the most downstream transverse level line was observed by the field party and verifies the positioning of this line on the image. The measured relative elevations along the lines indicated in the figure as well as the interpolated topography (Bindschadler and others, 1987b, fig. 6) agree very well with that inferred from the image. At the time the elevations were being measured, tiltmeters were used to search for evidence of grounding-line flexure. Diurnal flexure was measured at station E2 and at two sites 11 and 12 km northwest of E2 (1 and 2 km northwest of E2.3A), but not at a fourth site just 2 km northwest of E2 (Bindschadler and others, 1987b). These results draw attention to the fact that in the image the line from E2 to E2.3A straddles an area that appears slightly higher (more grounded?) than the adjacent ice. This interpretation is consistent with the tiltmeter results — the single case of no tilt occurs in the interior of this grounded area while the three locations where tilt was observed are at the flexing edge of this area.

Again, the possibility of temporal changes in grounding in this area must be considered. Bindschadler and others (1989) have calculated a rapid thickening rate (0.76 m a^{-1}) in the region upstream of Crary Ice Rise. The tiltmeter measurements were made in December 1984 and the SPOT image was collected in December 1989. At the thickening rate cited above, nearly 4 m of thickening would have occurred during this 5 year interval. Additional evidence is presented later that thickening has been taking place and that nearest the ice rise the thickening rates have been much higher. Rapid thickening could explain why, using 1984 data, E2 clustered with floating stations in a plot of ice thickness versus surface elevation (Bindschadler and others, 1987b, fig. 3). Station E2 lies very close to a thin embayment of shelf ice; this could allow sub-shelf water to penetrate close to E2 and cause the measured tilting.

There are many slightly curving features that appear in Figure 5 — most are concentrated in the lightly grounded zone downstream of a line between stations G2 and G8. Figure 6c shows elevations along a leveling line from station O toward C2 that crossed three such features (Bindschadler and others, 1988b). These features are troughs approximately 2 m deep without a corresponding ridge. Because the topographic character of these features is different from the flow stripes near station A2 as discussed earlier, their genesis is probably different. It is speculated here that the troughs are caused by "ruptures" in the subglacial till material and what is seen on the surface is a slumping of the ice over the opening in the till. This could provide an hydraulic connection between these areas and the sub-shelf waters and allow tidal forcings to penetrate the grounded areas along these filaments, making tiltmeter measurements misleading. This hypothesis provides another explanation for a grounded station E2 exhibiting tidally induced motions as discussed above. It is not expected that radar sounding would be sensitive to these subglacial gaps because they would be flush with the bottom of the ice but the ability to locate their position on the image provides the opportunity to re-examine radar soundings in these locations.

Also seen in Figure 5 are numerous crevassed areas. Most obvious is the broad band in the lower left of the figure. This is the termination of the snake: the north margin of Ice Stream B. At the extreme lower left is the edge of a large, roughly triangular-shaped rift known to exist at this location from earlier aerial photography. It appeared on the USGS map discussed earlier and probably also is responsible for the bottom crevasses detected by airborne-radar soundings (Jezek and Bentley, 1983).

Adjacent to the snake is another band of intense crevassing that stops suddenly at the grounding line. The abrupt cessation of this crevassing indicates that it probably is recent; otherwise, a downstream trail of partially buried crevasses would be expected. Their dominant orientation (angles roughly 30° clockwise from the flow direction) indicates lateral shear and longitudinal compression. Thus, these crevasses may be associated with an advance of the grounding line into this area. Such an advance would also help to reconcile the difference between the Shabtaie and Bentley (1987) grounding line and that shown in Figure 5. Shabtaie and Bentley's data were collected in 1984–85 and included two flight lines in this region (see their fig. 2). If their interpretation was valid for 1984–85, then the grounding line has advanced 20 km in just 5 years. However, Shabtaie and others (1989) have argued that the grounding line in this area is retreating.

Additional evidence for change in this area comes from a review of data collected on a traverse of the Ross Ice Shelf conducted during the International Geophysical Year, 1957–58 (Crary and others, 1962). Surface-

https://doi.org/10.3189/S0022143000016439 Published online by Cambridge University Press

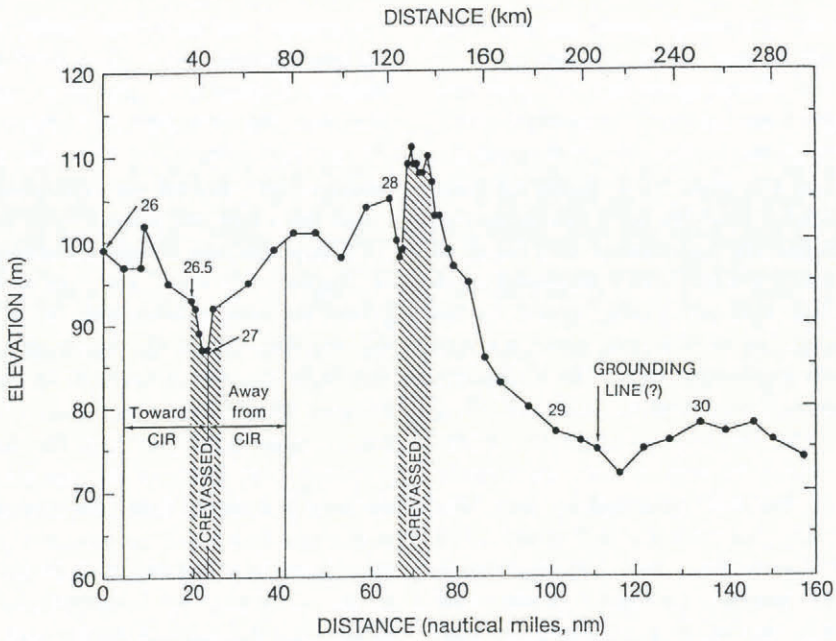

Fig. 7. Elevation profile measured in 1957 (IGY) by Crary and others (1962). Individual measurements are indicated by solid circles and connected with straight lines. Traverse route and station numbers are shown in Figure 5. At station 27 the field party turned around and retraced a 18.5 n.m. (nautical mile) distance, as discussed in the text. Shaded areas are where crevasses were observed. Possible grounding line is indicated.

elevation data were recorded nearly every hour at "short stations" by a three-altimeter method. At daily intervals, seismic investigations yielded data on ice thickness and sub-shelf water thickness. Figure 5 includes the position of their traverse route. The field party approached Crary Ice Rise from the upstream direction but doubled back when crevasses made advance impossible. Fortuitously, many of their data were taken in locations similar to where SCP data were collected.

Figure 7 is the IGY elevation profile from station 26 to beyond station 30. The repeatability of the section over which the party retraced its route (4–22.5 n.m. (nautical miles) and 22.5–41 n.m.) supports the accuracy of the measurements; however, there is little correspondence between the IGY-measured elevations and those inferred from the image. The expected location accuracy of the image is less than 500 m (0.25 n.m.) and the IGY positions were reported to the nearest 300 m (0.15 n.m.). The only difference between the two repeated legs of the IGY traverse is a 6 m rise measured while approaching Crary Ice Rise that was not measured while leaving the ice rise. Given the isolated nature of the finger of grounded ice at roughly this location, it is possible to believe that either small differences in the exact location of the measurement or location uncertainties could account for this difference. Impossible to explain, however, is the difference between the twice-measured decrease in elevation between stations 26 and 27 and the occurrence in the image of elevated, grounded ice beginning along this profile upstream of station 26.5. A similar discrepancy occurs between the more rapid elevation decrease measured in the IGY between stations 26.5 and 27 and the absence of any significant slope in the image in this area. Spatial variations in ice thickness could help resolve these discrepancies but, as mentioned earlier, Shabtaie (personal communication) measured no substantial variations in ice thickness between SCP stations E2 and E2.5. These findings will be combined with others presented later to suggest that, during the IGY, the area between stations 26 and 27 (with the possible exception of the single rise 9 n.m. downstream of station 26) was floating.

The absence of significant short-wavelength topographic variations on the eastward leg to IGY station 28 leaves little to compare with what is also a quiescent variation in image brightness. However, beyond station 28 the IGY party measured large, tightly spaced elevation variations and encountered numerous crevasses striking southeast–northwest (i.e. along the flow) into which snow tractors repeatedly fell (Crary and others, 1962). In the image, longitudinal ridges do occur in approximately the correct location but there are no crevasses. The nearest crevasses occur 10 km east of the IGY route but at about the correct distance along the route from station 28. The nearest open crevasses are located at least another 20 km farther to the northeast. The 10 m pixel resolution of the SPOT image should be sufficient for indicating the existence of any other crevasses in this vicinity.

Subsequent to this elevated, crevassed area, the surface elevation gradually decreased in a manner that suggests the grounding line was crossed between stations 29 and 30 (at 110 n.m.; Fig. 7). This interpretation differs slightly from that used by Shabtaie and Bentley (1987) to draw their grounding line—they chose the interval of maximum elevation change before station 29 (near 85 n.m.) (personal communication from S. Shabtaie). Believing that the dip immediately beyond 110 n.m. corresponds to the hinge-line valley (Stephenson and Doake, 1982; Thomas and others, 1988), the 110 n.m. position is the better choice. Unfortunately, the SPOT image does not extend to this location, but that part of the

IGY traverse included in Figure 5 indicates that grounded ice extends at least 50 km (25 n.m.) from station 28.

If Crary's field party left grounded ice after station 28, the question of when they first encountered grounded ice remains. Given the changes that must have taken place between the time of the SPOT image and the IGY data, the image cannot help answer this question. Nevertheless, the subtle nature of the current grounding "line" on the southern boundary of the ice plain allows speculation that grounded ice could have been encountered at approximately 52 n.m. while traveling eastward toward station 28.

The IGY measurements of ice thickness also supply considerable insight into former conditions of this area and enable a direct comparison of conditions derived from SCP measurements. Figure 8 reproduces part of a figure from the IGY report that plots ice thickness versus surface elevation. While the theoretical curve fits most of the station data (not shown), all of the stations nearest the Transantarctic Mountains (20–29) lie to the right of the flotation curve. This could be interpreted as an indication that these stations are grounded, but a more likely explanation is that the average column density for these stations is lower due to a higher accumulation rate caused by their proximity to the mountains (Crary and others, 1962, fig. 22). Shabtaie and Bentley (1987) re-examined the IGY seismic records and felt that the interpretation of the reflection from the bottom of the sub-shelf water cavity was ambiguous for many of the stations in this area. The station farthest to the right of the flotation curve in Figure 8, and therefore most likely to be grounded most firmly, is station 28.

There are two SCP stations that lie very close to former IGY positions. SCP station E2 is 3.4 km southeast of IGY station 26.5 and SCP station C1 is 1.4 km northeast of IGY station 26 (see Fig. 5). In 1984, the ice at E2 was measured by radar soundings to be 680 m thick (personal communication from S. Shabtaie). In 1957, the ice thickness at station 26.5 was measured seismically at

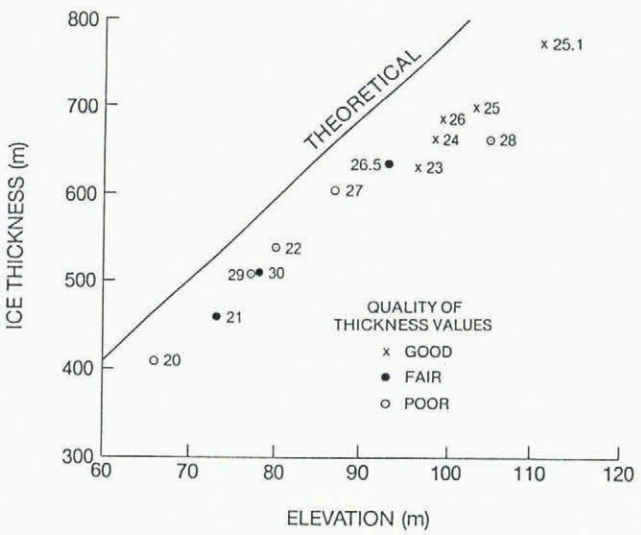

Fig. 8. Ice-thickness values obtained by seismic reflections versus surface elevations determined from multiple altimetry. Taken from Crary and others (1962). Only stations discussed in the text are shown.

631 m, an apparent thickening of 49 m. The second comparison cannot be as precise because no SCP measurement was made at C1 but there was a measurement made at station O, 15 km away, and these two stations were linked with an accurate optical level line. Station C1 is floating and station O is probably floating; the elevation profile between them does not suggest that a grounding line was crossed (see Fig. 6c) and no strand cracks were observed on the surface. Thus, the 5 m increase in surface elevation from O to C1 can be used to infer that in 1984 ice at C1 was 45 m thicker than at O, or 743 m. (The ice thickness at O was measured by Shabtaie (personal communication).) If station O was grounded, the thickness at C1 would be even greater. Comparing this best estimate of 743 m with the 1957 seismic measurement of 681 m at station 26 implies a thickening of 62 m. Thus, there appears to be solid evidence in this region for significant thickening of about 55 m over 27 years, or an average rate of 2 m a^{-1}. This is nearly three times the 0.76 m a^{-1} calculated by Bindschadler and others (1989) but this lower figure applied to a much wider area. The higher figure agrees better with detailed net mass-balance calculations that can better represent local effects (Bindschadler and others, 1993).

CRARY ICE RISE

Nowhere is the transience of the West Antarctic ice sheet more apparent than in the vicinity of Crary Ice Rise. It is a major feature of the Ross Ice Shelf rising nearly 50 m above the surrounding ice shelf. A number of detailed SCP studies have shown that major changes are taking place on and around it.

Shabtaie and Bentley's (1987) map of the ice rise, based on data collected from a few airborne-radar-sounding flights, revealed that the main ice rise was bounded on both transverse sides by additional patches of ice similar in radar signature to a grounded ice rise. From the radar data alone, it was not possible to determine whether these areas were actual ice rises, but the lack of a significant increase in the surface elevation suggested that they were not. Nevertheless, Jezek and Bentley (1983) noticed evidence of bottom crevasses in radar-sounding data taken downstream of these potentially grounded areas alongside Crary Ice Rise. Of the many flow measurements made on the ice shelf near Crary Ice Rise, only two sites occurred between the main ice rise and the adjacent areas suspected to be grounded. At both of these sites, RIGGS station H10 and lines extending from SCP station L1, the ice exhibited large (almost 10^{-2} a^{-1}), nearly pure shear. Deformation measurements at ice-shelf stations outside these areas also indicated a high shear component but nearly an order of magnitude lower (Bindschadler and others, 1988a). These data suggested that, while these adjacent areas may have been grounded, they certainly were not stagnant.

Additional information on these areas came from a map of crevasses, undulations and ruptures in the ice shelf made from a mosaic of aerial photography (Bindschadler and others, 1988a). This map delineated the spatial extent of most of these clutter-free areas. One area in particular, on the northeast side of Crary Ice Rise, was

https://doi.org/10.3189/S0022143000016439 Published online by Cambridge University Press

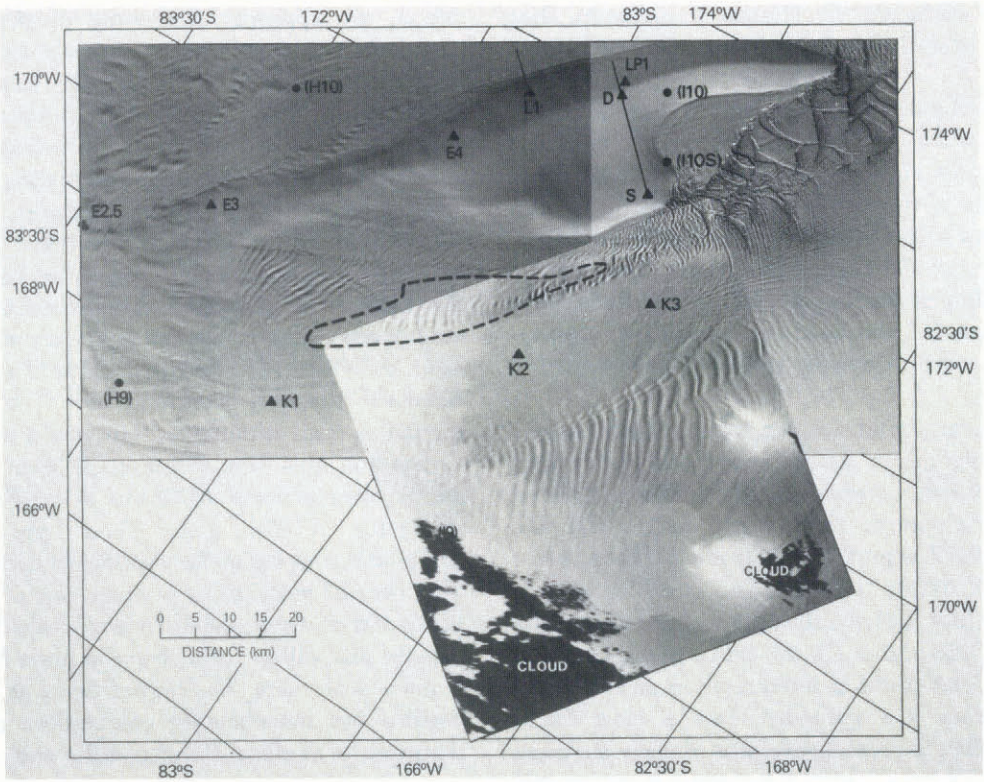

Fig. 9. Crary Ice Rise mosaic using three SPOT scenes. Solid circles and triangles are stations from RIGGS and SCP, respectively. Dashed line identifies raft discussed in the text. Vertical cross-section along line connecting stations D and S is shown in Figure 10.

separated from the ice rise by a band of intense shear crevasses over 6 km wide. Bindschadler and others (1988a) hypothesized that this "raft" of clutter-free ice had once been part of a larger Crary Ice Rise, had recently separated from the ice rise, and was being incorporated into the ice shelf. This interpretation is supported by the measurements at SCP stations K2 and K3, nearest the raft where there are significant tensile components of the strain-rate field oriented in the general direction necessary to pull the raft from the ice rise (see Bindschadler and others, 1988a, fig. 4). Confirmation of this raft's separation from the ice rise came by way of a measured velocity of 160 m a^{-1} from repeat geoceiver positions near the downstream tip of the raft (Bindschadler, unpublished). Earlier, Bindschadler and others (1988a) had predicted a velocity in the range 140–185 m a^{-1} based on velocity measurements adjacent to the area. Finally, by estimating the void space of crevasses between the raft and Crary Ice Rise, and dividing by the current velocity, Bindschadler and others (1988a) estimated that this separation might have occurred only 20 years ago and probably within the last 50 years.

Three SPOT images of Crary Ice Rise are mosaiced in Figure 9. From the mapping of the 1984 aerial photography, the general shape of the ice rise and many of the details of the flow around it were already known, but additional details can be seen in the imagery. The shading on the ice rise itself furnishes an excellent sense of its topographic shape. The solar illumination for the two images showing the ice rise is from the bottom of the figure, while the illumination for the third image (with the clouds) is from the left. The ridge on the downstream-pointing "finger" is pronounced; station D lies on the crest line. A lower dome centered on station S lies northwest of the ridge. A broad valley runs between these two features, ending in a large embayment of stagnant ice from which large rafts of ice are spalled as the ice shelf moves past the ice rise. Upstream from these major features the ice rise rapidly narrows, eventually merging with the ice plain near station E2.5. Bindschadler and others (1990, fig. 1) gave a coarse elevation map of Crary Ice Rise. Figure 10 is a downstream-looking cross-section through the ice rise, connecting stations D and S (radar data were supplied by S. Shabtaie). The flotation surface calculated from the bed elevations shows that the valley is just 20 m above hydrostatic equilibrium while the finger and dome are 75 and 50 m above flotation, respectively. The asymmetry between the surface and bed profiles is an indication of a non-equilibrium configuration as described by MacAyeal and Thomas (1980). From five additional airborne-radar-sounding transects of the ice rise (Blankenship, unpublished), it is known that the finger rests on a sloping bed for most of its length — also a non-equilibrium condition. Furthermore, the highest part of the bed (~280 m a.s.l.) underlies station S.

Stations D and S were the sites where vertical temperature profiles were measured and analyzed to determine the time since Crary Ice Rise first grounded (Bindschadler and others, 1990). Their analysis was based on the principle that the basal ice of an ice shelf receives much more heat than is available geothermally. Thus, when an ice shelf grounds, the bed will freeze and the entire ice column will cool. The time required for a complete thermal transition for ice a few hundred meters

https://doi.org/10.3189/S0022143000016439 Published online by Cambridge University Press

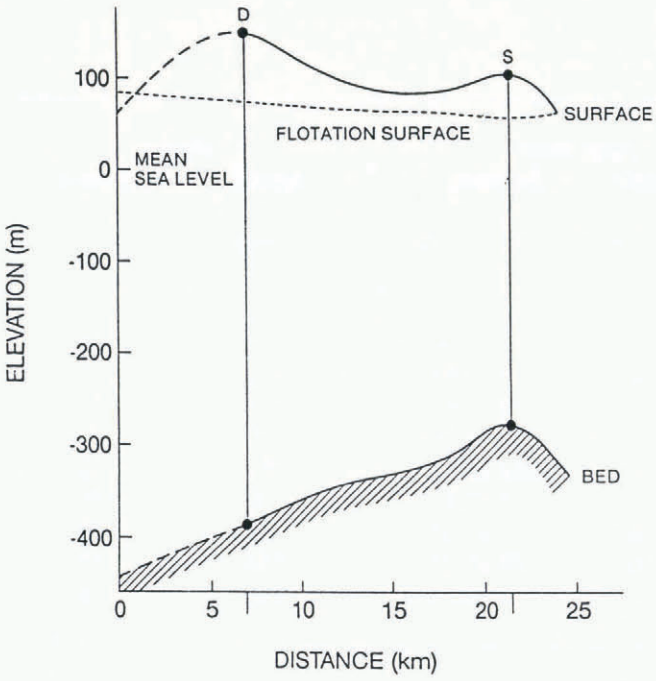

Fig. 10. Vertical cross-section along line between stations D and S on Crary Ice Rise (see Fig. 9). Surface was measured by optical leveling and is dashed where uncertain. Bed was measured by airborne-radar sounding (personal communication from S. Shabtaie). Flotation surface was calculated from the bed using a mean ice-column density of 850 kg m^{-3}.

thick takes thousands of years. During this transition period, there will be a transient, or intermediate, temperature condition which can be inverted through numerical models to determine the time of grounding. Site S was chosen because it overlaid the highest point in the bed, while site D was chosen because, as the highest point on the surface, it was believed to be the site of deepest ice. Each site was expected to have been occupied by grounded ice for the longest periods and, therefore, to provide maximum ages for their respective parts of the ice rise.

While the details of the analysis can be read in Bindschadler and others (1990), the results can be stated succinctly. The calculated grounding dates were surprisingly young; 1100 years ago at D and 580 years ago at S. Furthermore, the temperatures at and near the base at site S were so warm that the cooling process has probably only been taking place for the past 130 years. These ages establish that the Crary Ice Rise present today is not a relict feature from the last glacial maximum. However, this analysis leaves many other questions unanswered. The non-equilibrium shape of Crary Ice Rise remains unexplained. The finger may owe its existence to grounding that originated farther downstream in an area beyond the current ice rise; detailed bathymetry of this area does not exist. The fact that the oldest grounding was found not to occur on the highest part of the bed could be the result of a strong thickness gradient (increasing toward the Transantarctic Mountains) that is seen in the ice shelf (Jezek and Bentley, 1983). Finally, there is evidence from flow stripes seen in other satellite imagery that the region southwest of Crary Ice Rise has had a very turbulent past (Casassa and Turner, 1991).

Support for the conclusion that rapid changes are still occurring around the ice rise came from an extension to the net mass-balance calculations of MacAyeal and others (1987). While these authors showed that the overall mass balance in the vicinity of the ice rise was quite small ($0.14 \pm 0.09\,m\,a^{-1}$), Bindschadler and others (1989) showed that the regional pattern of net mass balance indicated dramatic changes were under way. On the downstream side, calculated thinning rates exceeded $1.0\,m\,a^{-1}$ (ice equivalent), while on the upstream and Transantarctic Mountains sides, intensive thickening was taking place at rates of $0.60\,m\,a^{-1}$ and higher. Without sub-shelf measurements, these calculations assumed no basal melting or freezing but the rates are large enough that basal processes would not destroy the overall pattern. These results indicated that the ice rise must be migrating upstream. Attempts to determine the rate of migration were based on the single available measurement of bed slope near the upstream edge of Crary Ice Rise and produced an estimate of $380\,m\,a^{-1}$.

The upstream "tail" of the ice rise (Fig. 9) is very much lower than either the finger or the dome. In earlier maps of Crary Ice Rise (e.g. Thomas and others, 1984), this tail was ignored and a much shorter Crary Ice Rise was indicated. This was probably an error and not representative of a real change in the ice rise. The imagery does reveal a complex pattern of surface relief in the areas surrounding this tail: small isolated patches of grounded ice populate the south (upper left) corner of the image and a strong banded pattern delineates the "bow wave" associated with the flow of ice around the upstream tip of the ice rise. Included within the grounded area in the northeast of Figure 9 is the location of RIGGS station H9. As with station G8, the velocity at this location is calculated to have decreased 28% in 11 years (Stephenson and Bindschadler, 1988), although the authors of that paper suggested that the proximity of crevasses may introduce error into the interpolation scheme used in their analysis. Nevertheless, these errors do not compromise the result that substantial deceleration has occurred, the cause of which is either the increased thickening and/or the upstream migration of Crary Ice Rise, both discussed earlier.

Much of the area to the northeast of Crary Ice Rise shown in Figure 9 was included in the aerial photographic coverage but the imagery extends coverage farther to reveal additional complexity. In order of increasing distance from the ice rise, there is a rumpled area associated with the raft described above and the shearing flow past the grounded ice rise, a smooth area with a set of diverging flow stripes at the downstream end of the image, a band of irregularly spaced rumples oriented roughly transverse to the flow and, finally, a smoother region of ice oriented at an angle to the long axis of Crary Ice Rise and containing subtle flow stripes and transverse scars. Rumpled surfaces suggest grounded ice. The rumpled band farthest from the ice rise occurs in a region that falls between the RIGGS radar-sounding flights (see Bentley and others, 1984), so it may well have escaped detection until now. The two smoother regions are most likely floating ice shelf and the orientation of the one farthest from Crary Ice Rise indicates converging

https://doi.org/10.3189/S0022143000016439 Published online by Cambridge University Press

Table 1. SPOT scenes of ice plain and Crary Ice Rise area

Scene ID# (see footnote)	*Figure*	*Scene center*		*Sun*	
		Latitude	*Longitude*	*Azimuth*	*Elevation*
		° ′ ″S	° ′ ″W	° true	°
108557289011012273 92P	2	84 25 29	152 54 04	149	17
10855708901101227391P	2	83 51 12	149 25 47	146	17
10825728902071329472P	4	84 13 10	159 18 57	141	11
10795698912021620472P	5	83 37 03	161 36 26	96	21
10785708912021620562P	5	83 44 12	166 04 13	101	21
10745688912021801421P	9	83 11 48	169 58 11	80	23
10725678912021801422P	9	82 50 44	171 45 35	82	23
10735678901231318401P	9	82 49 04	169 43 27	154	13
10885738802181356131P	–	82 27 32	147 14 17	123	9

Note: Scene ID# is composed of:

digit 1:	Number of SPOT satellite.
digits 2–4 and 5–7:	K and J (geographic indices used by SPOT).
digits 8–13:	Date (YYMMDD format).
digits 14–19:	GMT (HHMMSS format).
digit 20:	Camera number.
digit 21:	Mode (P = Panchromatic).

flow around the downstream side of the rumpled zone. No RIGGS or SCP velocities exist in this area, so it cannot be said at this point whether this pattern of surface features is consistent with the current velocity field.

MacAyeal and others (1987) computed the forces exerted on Crary Ice Rise and the surrounding ice shelf by the ice upstream to be 4.04×10^{13} N. Half of this force was attributed to the ice rise and the other half to the ice shelf. This total force is the back pressure referred to in the theory of Thomas (1973). From Bindschadler and others (1987a), the total driving force on the ice plain from DNB to H2 can be calculated as 3×10^{13} N. Modifying these numbers to extend the ice-plain area to Crary Ice Rise increases the total driving force to 4.5×10^{13} N. Additional resistance from side shear could be as much as 1.5×10^{13} N, again using the data from Bindschadler and others (1987a), but the effect of strain softening would reduce this number. Thus, the combination of back pressure from Crary Ice Rise and side shear from the snake are sufficient to balance the driving force on the ice plain. Although the back-pressure term dominates on the ice plain, the effect of Crary Ice Rise probably does not extend farther upstream. This result also suggests that basal shear does not significantly resist the flow of the ice plain.

ICE STREAM C

SCP investigations were located in this area because Ice Stream C afforded glaciologists a unique view of an ice stream that was no longer active. The studies of Ice Stream C have been largely directed towards making comparisons with its active neighbor, Ice Stream B. It is hoped that, eventually, such comparisons will supply clues to the cause of the cessation of fast motion and requirements for the maintenance of active ice streams. Because the behavior of the bed is most critical in determining whether the ice stream flows rapidly or slowly, most of the critical investigations involve sounding radar and seismic methods (Blankenship and others, 1987; Jacobel and others, 1988). Because of low flow velocities, the overall net mass balance of the ice stream is strongly positive (Shabtaie and Bentley, 1987). Eventually, the positive mass balance will force a dynamic response, possibly including a return to active streaming flow.

In the meantime, the studies of flow in the mouth of Ice Stream C, when taken by themselves, yield few dramatic results. Both near the grounding line as well as upstream in the middle of the ice stream, flow velocities are well below 10 m a^{-1} and strain rates, below 10^{-5} a^{-1}, both near the limit of uncertainty (Bindschadler and others, 1987b; Whillans and others, 1987).

The most intriguing analysis in this area involved a re-measurement of the positions of a network of survey markers established in 1975 at RIGGS station H5 (Thomas and others, 1988). This network straddled the grounding line and the SCP re-measurement allowed the discovery that the grounding line had retreated approximately 300 m in 11 years, an average of 27 m a^{-1}. This retreat results from grounding-line thinning driven by the continued thinning of the ice shelf. Satellite imagery has facilitated the identification of the grounding line and

provides a means of monitoring its position as retreat continues (Bindschadler and Vornberger, 1990; Stephenson and Bindschadler, 1990).

Shabtaie and Bentley (1987) used the burial depth of crevasses to estimate that Ice Stream C ceased rapid motion 250 years ago. More recent data have been used to revise this date to 130 years ago (Retzlaff and Bentley, 1990). In Landsat imagery, Stephenson and Bindschadler (1990) found a series of knolls on the ice shelf that are in line with the northern margin of the ice stream and are separated from the present grounding line by roughly 2 km. If this separation began about 200 years ago, the average retreat rate of the grounding line at the north margin is only $10\,m\,a^{-1}$ compared with the $27\,m\,a^{-1}$ calculated farther south at H5. Finally, Thomas and others (1988) argued that there may have been an ice plain extending 150 km downstream of the present grounding line and that in the initial stages of retreat, the rate of retreat was $300\,m\,a^{-1}$ or more over an area of much shallower basal slopes, and that only in the final stages would the retreat have fallen to values such as those observed during the RIGGS and SCP. Reconciliation of these various estimates cannot be attempted without further data.

SUMMARY

The results of the SCP have made major contributions to our understanding of the behavior, history and future of the Siple Coast ice streams and the region of interaction between the ice streams and the Ross Ice Shelf. Perhaps the most amazing discovery is that large changes in configuration, ice thickness and velocity can take place on very short time-scales. The 20% deceleration of the ice plain took place in just a decade; the separation of the raft from Crary Ice Rise occurred in the last few decades; the cessation of fast flow of Ice Stream C happened 130 years ago; the grounding of the present-day Crary Ice Rise is only a few centuries old; and ice thicknesses are changing at rates of a few $cm\,a^{-1}$ throughout the region and at a few sites at rates of over $1\,m\,a^{-1}$.

Clearly, there is still much to be learned. There is every reason to expect that many of the temporal changes listed above are inter-related. The linking of these separate events into a comprehensive history of the region will increase our ability to predict the future of this area. Numerical models will be required to simulate these complex interactions. These are the challenges that lie in future research of this region.

This paper has taken advantage of satellite imagery to critique past analyses of SCP data and expand the results. The images used are limited in their spatial coverage but the utility of the method is undeniable. Additional coverage can be expected to provide further insight as to the behavior and history of other areas, both in the Siple Coast region and in other parts of Antarctica. Sequential image coverage will replace the need for many of the types of investigation conducted during the SCP and help guide future field studies to the regions of greatest dynamic change.

ACKNOWLEDGEMENTS

The Siple Coast Project has been extremely successful due to the unselfish contributions of all its many participants. Principal investigators involved in the work in the areas discussed in this paper are C. Bentley, D. MacAyeal and I. Whillans. Many others assisted in the collection of the data presented in this paper, often under very difficult field conditions. Those who contributed additionally in the analysis of these are S. Stephenson, P. Vornberger and E. Roberts; I thank them all. Cloud-cover estimates were provided by the U.S. Meteorological Office at McMurdo Station operated by the U.S. Naval Support Force Antarctica and were instrumental in the identification of the SPOT images used. Funding support was provided by U.S. National Science Foundation grant DPP-8614407.

REFERENCES

Alley, R.B. 1993. In search of ice-stream sticky spots. *J. Glaciol.*, **39**(133), 447–454.

Alley, R.B. and I.M. Whillans. 1991. Changes in the West Antarctic ice sheet. *Science*, **254**(5034), 959–963.

Alley, R.B., D.D. Blankenship, S.T. Rooney and C.R. Bentley. 1989. Sedimentation beneath ice shelves — the view from Ice Stream B. *Mar. Geol.*, **85**(2/4), 101–120.

Bentley, C.R. 1984. The Ross Ice Shelf Geophysical and Glaciological Survey (RIGGS): introduction and summary of measurements performed. *Antarct. Res. Ser.*, **42**, 1–20.

Bindschadler, R.A. and P.L. Vornberger. 1990. AVHRR imagery reveals Antarctic ice dynamics. *EOS*, **71**(23), 741–742.

Bindschadler, R.A. and T.A. Scambos. 1991. Satellite-image-derived velocity field of an Antarctic ice stream. *Science*, **252**(5003), 242–246.

Bindschadler, R.A., S.N. Stephenson, D.R. MacAyeal and S. Shabtaie. 1987a. Ice dynamics at the mouth of Ice Stream B, Antarctica. *J. Geophys. Res.*, **92**(B9), 8885–8894.

Bindschadler, R.A., D.R. MacAyeal and S.N. Stephenson. 1987b. Ice stream–ice shelf interaction in West Antarctica. *In* Veen, C.J. van der and J. Oerlemans, *eds. Dynamics of the West Antarctic ice sheet.* Dordrecht, etc., D. Reidel Publishing Co., 161–180.

Bindschadler, R.A., E.P. Roberts and D.R. MacAyeal. 1989. Distribution of net mass balance in the vicinity of Crary Ice Rise, Antarctica. *J. Glaciol.*, **35**(121), 370–377.

Bindschadler, R.A., E.P. Roberts and A. Iken. 1990. Age of Crary Ice Rise, Antarctica, determined from temperature-depth profiles. *Ann. Glaciol.*, **14**, 13–16.

Bindschadler, R.A., P.L. Vornberger and S. Shabtaie. 1993. The detailed net mass balance of the ice plain on Ice Stream B, Antarctica: a geographic information system approach. *J. Glaciol.*, **39**(133), 471–482.

Blankenship, D.D., C.R. Bentley, S.T. Rooney and R.B. Alley. 1987. Till beneath Ice Stream B. 1. Properties derived from seismic travel times. *J. Geophys. Res.*, **92**(B9), 8903–8911.

Blankenship, D.D., S.T. Rooney and R.B. Alley. 1990. Glaciolgical influences on sedimentological processes in the Ross Embayment. *In* Cooper, A.K. and P.N. Webb, *convenors.* International Workshop on Antarctic Offshore Seismic Stratigraphy (ANTOSTRAT): overview and extended abstracts. *USGS Open File Report* 90–309.

Casassa, G and J. Turner. 1991. Dynamics of the Ross Ice Shelf. *EOS*, **72**(44), 473–481.

Crary, A.P., E.S. Robinson, H.F. Bennett and W.W. Boyd. 1962. Glaciological studies of the Ross Ice Shelf, Antarctica, 1957–1960. *IGY Glaciol. Rep. Ser.* 6.

Englehardt, H., N. Humphrey, B. Kamb and M. Fahnestock. 1990. Physical conditions at the base of a fast moving Antarctic ice stream. *Science*, **248**(4951), 57–59.

Hughes, T.J. 1973. Is the West Antarctic ice sheet disintegrating? *J. Geophys. Res.*, **78**(33), 7884–7910.

Jacobel, R.W. and R.A. Bindschadler. 1993. Radar studies in the mouths of Ice Streams D and E, Antarctica. *Ann. Glaciol.*, **17**, 262–268.

Jacobel, R. W., S. K. Anderson and D. F. Rioux. 1988. A portable digital data-acquisition system for surface-based ice-radar studies. *J. Glaciol.*, **34**(118), 349–354.

Jezek, K. C. 1984. A modified theory of bottom crevasses used as a means for measuring the buttressing effect of ice shelves on inland ice sheets. *J. Geophys. Res.*, **89**(B3), 1925–1931.

Jezek, K. C. and C. R. Bentley. 1983. Field studies of bottom crevasses in the Ross Ice Shelf, Antarctica. *J. Glaciol.*, **29**(101), 118–126.

MacAyeal, D. R. 1992. The basal stress distribution of ice stream E, Antarctica, inferred by control methods. *J. Geophys. Res.*, **97**(B1), 595–603.

MacAyeal, D. R. and R. H. Thomas. 1980. Ice-shelf grounding: ice and bedrock temperature changes. *J. Glaciol.*, **25**(93), 397–400.

MacAyeal, D. R., R. A. Bindschadler, S. Shabtaie, S. N. Stephenson and C. R. Bentley. 1987. Force, mass and energy budgets of the Crary Ice Rise complex, Antarctica. *J. Glaciol.*, **33**(114), 218–230. [Correction in *J. Glaciol.*, **35**(119), 1989, 151–152.]

MacAyeal, D. R., R. A. Bindschadler, K. C. Jezek and S. Shabtaie. 1988. Can relict crevasse plumes on Antarctic ice shelves reveal a history of ice-stream fluctuation? *Ann. Glaciol.*, **11**, 77–82.

Rees, W. G. and J. A. Dowdeswell. 1988. Topographic effects on light scattering from snow. *IGARSS'88. Proceedings, 13–16 Sept., 1988. ESA SP-284. IEEE 88CH2497-6.*

Retzlaff, R. and C. R. Bentley. 1990. Buried surface crevasses in Ice Stream C detected by short-pulse radar sounding. [Abstract.] *EOS*, **71**(43), 1310.

Robertson, J. D. and C. R. Bentley. 1990. Seismic studies on the grid-western half of the Ross Ice Shelf: RIGGS I and RIGGS II. *Antarct. Res. Ser.*, **42**, 55–86.

Rose, K. E. 1979. Characteristics of ice flow in Marie Byrd Land, Antarctica. *J. Glaciol.*, **24**(90), 63–75.

Shabtaie, S. and C. R. Bentley. 1987. West Antarctic ice streams draining into the Ross Ice Shelf: configuration and mass balance. *J. Geophys. Res.*, **92**(B2), 1311–1336.

Shabtaie, S. and C. R. Bentley. 1988. Ice-thickness mass of the West Antarctic ice streams by radar sounding. *Ann. Glaciol.*, **11**, 126–136.

Shabtaie, S., C. R. Bentley, R. A. Bindschadler and D. R. MacAyeal. 1988. Mass-balance studies of Ice Streams A, B, and C, and possible surging behavior of Ice Stream B. *Ann. Glaciol.*, **11**, 137–149.

Shabtaie, S., D. G. Schultz and C. R. Bentley. 1989. Grounding-line retreat of Ice Stream B, Antarctica. (Abstract.) *Ann. Glaciol.*, **12**, 208.

Siple Coast Project Steering Committee. 1988. *Science plan for the Siple Coast Project.* Available from Librarian, Goldthwait Polar Library, Byrd Polar Research Center, Ohio State University, Columbus, OH.

Stephenson, S. N. and R. A. Bindschadler. 1988. Observed velocity fluctuations on a major Antarctic ice stream. *Nature*, **334**(6184), 695–697.

Stephenson, S. N. and R. A. Bindschadler. 1990. Is ice-stream evolution revealed by satellite imagery? *Ann. Glaciol.*, **14**, 273–277.

Stephenson, S. N. and C. S. M. Doake. 1982. Dynamic behaviour of Rutford Ice Stream. *Ann. Glaciol.*, **3**, 295–299.

Thomas, R. H. 1973. The creep of ice shelves: theory. *J. Glaciol.*, **12**(64), 45–53.

Thomas, R. H., D. R. MacAyeal, D. H. Eilers and D. R. Gaylord. 1984. Glaciological studies on the Ross Ice Shelf, Antarctica, 1973–1978. *Antarct. Res. Ser.*, **42**, 21–53.

Thomas, R. H., S. N. Stephenson, R. A. Bindschadler, S. Shabtaie and C. R. Bentley. 1988. Thinning and grounding-line retreat on Ross Ice Shelf. *Ann. Glaciol.*, **11**, 165–172.

Vaughan, D. G. and C. S. M. Doake. 1989. Comparison between SPOT and Landsat imagery of Rutford Ice Stream, Antarctica. (Abstract.) *Ann. Glaciol.*, **12**, 217.

Vaughan, D. G., C. S. M. Doake and D. R. Mantripp. 1988. Topography of an Antarctic ice stream. *In SPOT-1 image utilization, assessment, results.* Toulouse, CNES Cepadues-Editions, 167–174.

Vornberger, P. L. and I. M. Whillans. 1986. Surface features of Ice Stream B, Marie Byrd Land, West Antarctica. *Ann. Glaciol.*, **8**, 168–170.

Whillans, I. M. 1987. Force budget of ice sheets. *In* Veen, C. J. van der and J. Oerlemans, *eds. Dynamics of the West Antarctic ice sheet.* Dordrecht, etc., D. Reidel Publishing Co., 17–36.

Whillans, I. M. and R. A. Bindschadler. 1988. Mass balance of Ice Stream B, West Antarctica. *Ann. Glaciol.*, **11**, 187–193.

Whillans, I. M., J. Bolzan and S. Shabtaie. 1987. Velocity of Ice Streams B and C, Antarctica. *J. Geophys. Res.*, **92**(B9), 8895–8902.

The accuracy of references in the text and in this list is the responsibility of the author, to whom queries should be addressed.

MS received 7 October 1991 and in revised form 23 February 1993